THE JOURNAL OF BIOLOGICAL CHEMISTRY VOL. 290, NO. 16, pp. 9986–9999, April 17, 2015

Influence of Oxidized Purine Processing on Strand Directionality of Mismatch Repair*

Received for publication, December 2, 2014, and in revised form, February 12, 2015 Published, JBC Papers in Press, February 18, 2015, DOI 10.1074/jbc.M114.629907

Simone Repmann, Maite Olivera-Harris, and Josef Jiricny[1]

From the Institute of Molecular Cancer Research of the University of Zurich and the Swiss Institutes of Technology Zurich, Winterthurerstrasse 190, 8057 Zurich, Switzerland

Background: We studied the interplay between base excision repair (BER) of 8-oxoguanine (G^O) and mismatch repair (MMR).
Results: BER and MMR interact during the processing of G^O/A but not G^O/C mispairs.
Conclusion: BER of G^O-containing lesions appears to be regulated.
Significance: BER intermediates were believed to be unavailable to other pathways of DNA metabolism. This hypothesis may be incorrect.

Replicative DNA polymerases are high fidelity enzymes that misincorporate nucleotides into nascent DNA with a frequency lower than [1/10^5], and this precision is improved to about [1/10^7] by their proofreading activity. Because this fidelity is insufficient to replicate most genomes without error, nature evolved postreplicative mismatch repair (MMR), which improves the fidelity of DNA replication by up to 3 orders of magnitude through correcting biosynthetic errors that escaped proofreading. MMR must be able to recognize non-Watson-Crick base pairs and excise the misincorporated nucleotides from the nascent DNA strand, which carries by definition the erroneous genetic information. In eukaryotes, MMR is believed to be directed to the nascent strand by preexisting discontinuities such as gaps between Okazaki fragments in the lagging strand or breaks in the leading strand generated by the mismatch-activated endonuclease of the MutL homologs PMS1 in yeast and PMS2 in vertebrates. We recently demonstrated that the eukaryotic MMR machinery can make use also of strand breaks arising during excision of uracils or ribonucleotides from DNA. We now show that intermediates of MutY homolog-dependent excision of adenines mispaired with 8-oxoguanine (G^O) also act as MMR initiation sites in extracts of human cells or *Xenopus laevis* eggs. Unexpectedly, G^O/C pairs were not processed in these extracts and failed to affect MMR directionality, but extracts supplemented with exogenous 8-oxoguanine DNA glycosylase (OGG1) did so. Because OGG1-mediated excision of G^O might misdirect MMR to the template strand, our findings suggest that OGG1 activity might be inhibited during MMR.

To improve the fidelity of DNA replication, mismatch repair (MMR)[2] must be able to detect base/base mismatches and small insertion/deletion loops that escaped the proofreading activity of the replicative polymerases and direct their excision and resynthesis activity to the nascent strand, which carries by definition the erroneous genetic information. In Gram-negative bacteria such as *Escherichia coli*, the newly synthesized strand remains transiently unmethylated on adenines within GATC sequences. Mismatch-activated MutS-MutL complex licenses MutH to incise the unmethylated GATC, which allows the loading of the UvrD helicase together with one of several exonucleases. This leads to the degradation of the error-containing strand from the MutH-catalyzed nick toward and some distance past the mismatch to generate a single-stranded gap that is subsequently filled in by polymerase III. The remaining nick is sealed by DNA ligase (1–3).

In eukaryotes, DNA methylation is not used in strand discrimination during MMR. Instead, the nascent strand is distinguished from the template by transient discontinuities such as gaps between Okazaki fragments in the lagging strand. The leading strand contains no such discontinuities other than the 3′ terminus. Because the only MMR-associated exonuclease identified to date, EXO1, has an obligate 5′ to 3′ polarity, it appeared unlikely that MMR would use the 3′ terminus of the primer strand for initiation. However, seminal work from Modrich and co-workers (4, 5) demonstrated that association of the mismatch-activated MutLα (a heterodimer of MLH1 and PMS2) with proliferating cell nuclear antigen bound at the 3′ terminus activates a cryptic endonuclease in the PMS2 subunit, which introduces nicks into the newly synthesized strand and thus provides EXO1 with entry sites where 5′ to 3′ degradation of the error-containing strand can initiate.

While studying the involvement of MMR in somatic hypermutation, which is triggered by activation-induced cytidine deaminase that converts cytosines to uracils at the immunoglobulin locus of activated B cells (6), we discovered that the MMR system can hijack strand breaks generated by the base excision repair (BER) system during uracil removal for the purpose of strand discrimination (7). This was unexpected because BER was thought to be a concerted process in which the strand break generated by apurinic endonuclease (APE1) after removal of the aberrant base is not available for other processes of

* This work was supported by Swiss National Science Foundation Grants 310030B-133123 and 31003A-149989 and European Research Council Grant "MIRIAM" 294537.
[1] To whom correspondence should be addressed. Tel.: 41-44-635-3450; Fax: 41-44-635-3484; E-mail: jiricny@imcr.uzh.ch.
[2] The abbreviations used are: MMR, mismatch repair; MYH, MutY homolog; G^O, 8-oxoguanine; OGG1, 8-oxoguanine DNA glycosylase; BER, base excision repair; MTH1, MutT homolog 1; A^O, 2-hydroxyadenine; APE1, apurinic endonuclease 1; TFIIH, transcription factor II H.

DNA metabolism (8). In later experiments, we showed that breaks generated during the RNase H2-catalyzed removal of ribonucleotides misincorporated into DNA during replication can also be utilized by MMR as strand discrimination signals (9).

The above experiments suggested that strand breaks arising during different processes of DNA metabolism may be hijacked by MMR. Although this might lead to improved replication fidelity when breaks in the nascent DNA strand were involved, the opposite would be true if breaks in the template strand were used to direct the MMR process. To gain novel insight into this phenomenon, we set out to examine the interplay between MMR and oxidative DNA damage metabolism because BER-mediated processing of oxidized DNA could potentially take place on both nascent and template strands.

Depending on cell type, human genomes have been estimated to harbor steady-state levels of the major product of DNA oxidation, 2′-deoxy-8-oxoguanosine, ranging between 1000 and 100,000 residues (10–12). This nucleoside can be present in DNA in two distinct contexts: either paired with deoxycytidine or mispaired with deoxyadenosine because the base, 8-oxoguanine (G^O), can adopt either an *anti* or a *syn* conformation about the glycosidic bond (13, 14). Thus, although oxidation of double-stranded DNA gives rise solely to G^O/C pairs in which G^O is in the *anti* conformation, the replicative polymerases α, δ, and ϵ could insert either a C opposite *anti*-G^O to form a Watson-Crick-like G^O/C base pair or an A opposite *syn*-G^O to form a Hoogsteen G^O/A mispair (15–17).

Oxidation also affects the nucleotide pool where it generates dG^OTP. However, because this nucleotide is hydrolyzed by MutT homolog 1 (MTH1) protein to dG^OMP (18–20), G^O should not be incorporated into the nascent DNA strand. Thus, in newly replicated DNA, all G^O residues should be in the template strand, and all As mispaired with G^O should be in the nascent strand. This point is key to our understanding of the potential interplay between oxidative damage processing and MMR.

G^O/C base pairs are addressed primarily by 8-oxoguanine DNA glycosylase (OGG1), a glycosylase/lyase that removes the oxidized base and cleaves the sugar-phosphate backbone to initiate a BER process that ultimately replaces the oxidized nucleotide with a dGMP (13). G^O/As are not addressed by OGG1; they are recognized by the MutY homolog (MYH) glycosylase, which removes the mispaired adenines to initiate a BER process that inserts Cs opposite the oxidized guanines. The G^O/Cs arising in this way can then be repaired later to G/C by OGG1-dependent BER (21, 22). Thus, if MMR were to use breaks generated during MYH-initiated BER of G^O/As, these discontinuities would be in the nascent strand, and their hijacking by MMR might improve the efficiency of the latter process. In contrast, incisions made during OGG1-initiated BER of G^O/Cs would be in the template strand where they would not only misdirect the mismatch repair process to the wrong strand but where they could also give rise to double strand breaks that could cause replication fork collapse.

In an attempt to learn whether MMR utilized strand breaks arising during MYH- and/or OGG1-initiated BER processes, we generated substrates containing a single nick (a *bona fide* strand discrimination signal), a G^O/A mispair, or a G^O/C pair and studied the efficiency and directionality of MMR-catalyzed repair of a G/T mismatch situated in the vicinity. We show that, in extracts of human cells or *Xenopus laevis* eggs, the MMR excision machinery can use strand breaks arising upon MYH-catalyzed removal of adenines from G^O/A mispairs as initiation sites for exonucleolytic degradation of error-containing strands on circular heteroduplex substrates. A similar phenomenon was not observed either on G^O/C-containing heteroduplexes or on substrates containing 2-hydroxyadenine (A^O), another product of purine oxidation (12), even though A^O/C and A^O/G mispairs were reported previously to be addressed by MYH (23, 24).

EXPERIMENTAL PROCEDURES

Restriction Enzymes

All restriction enzymes were purchased from New England Biolabs.

Recombinant Proteins

GST-tagged MYH was expressed from the pET41a-MYH expression vector (a gift from Dr. Barbara van Loon) and partially purified using glutathione-Sepharose beads (GE Healthcare) as described previously (25). In a second purification step, eluates were loaded onto a HiTrap™ Heparin HP column (GE Healthcare), which was then washed with 10 column volumes of wash buffer (30 mM Tris-HCl, pH 8, 0.1 mM EDTA, 10% glycerol, 1 mM DTT, 50 mM NaCl) at a flow rate of 0.5 ml/min. Elution was performed using a salt gradient (50–600 mM NaCl). MYH-GST was eluted with 400–500 mM NaCl. The active fractions were identified using a MYH nicking assay, pooled, aliquoted, and stored at −80 °C. Recombinant APE1 was purchased from New England Biolabs. Recombinant OGG1 was a kind gift from Barbara van Loon. Recombinant OGG1-GST was purchased from Trevigen (4130-100-EB). Recombinant MutLα and MutSα were expressed and purified in our laboratory as described previously (26).

The expression constructs for human geminin (geminin-pET28) and p27 (p27-pET21) were a kind gift from Yoshi Hashimoto and Vincenzo Costanzo. Briefly, protein expression was induced with 0.5 mM isopropyl 1-thio-β-D-galactopyranoside in BL21 cells (Invitrogen) grown at 37 °C. The cell pellets were resuspended in 20 mM Tris-HCl, pH 7.5, 500 mM KCl, 10% glycerol, 1 mM β-mercaptoethanol, 0.1% Nonidet P-40, and PMSF for lysis. After cell disruption and centrifugation of cell debris and membranes, the soluble fraction containing 10 mM imidazole was loaded onto a nickel-chelating column, which was then washed with 5–25 mM imidazole. The protein was eluted with a gradient of 50–300 mM imidazole. Fractions containing the desired polypeptides were pooled and dialyzed against EB buffer (100 mM KCl, 2.5 mM $MgCl_2$, 50 mM HEPES-KOH, pH 7.5, 10% glycerol).

Cell Culture

HCT116 (MutLα-deficient) and HCT116 + chromosome 3 (MutLα-proficient) cells were obtained from Richard Boland (27) and were cultured in McCoy's 5a medium (Gibco) supplemented

TABLE 1

Oligonucleotide primers used to generate the MMR substrates

The SalI (GTCGAC) and AclI (AACGTT) restriction sites are highlighted in bold and gray, respectively. PvuI restriction sites (CGATCG) are italicized, and mispaired residues are underlined.

Substrate	Oligonucleotide primer (5' to 3')
G/T[a or b]	CCAGACGTCT**GTC**GACGTT**GGGAAGCTTGAG**
T/G[c]	CCAGACGTCT**GTTGAC**GTTGGGAAGCTTGAG
G^O/A[b]	GAATTGTAAG^OACGAACACTATAGGGCGAATTGGCGGCCGCGATCTGATCAGATCCAGACGTCTGTCAACGTTGGGAAGCTTGAG
G^O/C[a]	GAATTGTAATACG^OAACACTATAGGGCGAATTGGCGGCCGCGATCTGATCAGATCCAGACGTCTGTCAACGTTGGGAAGCTTGAG
G^O/A-G/T[b]	GAATTGTAAG^OACGAACACTATAGGGCGAATTGGCGGCCGCGATCTGATCAGATCCAGACGTCT**GTCGAC**GTTGGGAAGCTTGAG
G^O/C-G/T[a]	GAATTGTAATACG^OAACACTATAGGGCGAATTGGCGGCCGCGATCTGATCAGATCCAGACGTCTGTC**GACGTT**GGGAAGCTTGAG
A^O/G-T/G[c]	GGGAAGGG*CGATA*^{O}*G*GTGCGGGCCTC and CCAGACGTCT**GTTGAC**GTTGGGAAGCTTGAG
A^O/C-T/G[c]	GGGAAGGG*CA*^{O}*ATCG*GTGCGGGCCTC and CCAGACGTCT**GTTGAC**GTTGGGAAGCTTGAG
A/T[a]	CCAGACGTCTGTCAACGTTGGGAAGCTTGAG
G/C[c]	CCAGACGTCT**GTCGAC**GTTGGGAAGCTTGAG

[a] Template was pRichi-2850topAclI.
[b] Template was pRichi-2850botAclI.
[c] Template was pRichi-2850topSalI.

with 10% bovine calf serum (Gibco). The medium for the chromosome 3-complemented cell line was supplemented with 400 μg/ml G418. LoVo (MutSα-deficient) cells were grown in DMEM (Gibco) supplemented with 10% bovine calf serum. All media additionally contained 1% penicillin/streptomycin.

Nuclear Extracts of Human Cells

Nuclei were isolated as described previously (28), resuspended in ⅓ of their packed volume in cold extraction buffer (25 mM HEPES-KOH, pH 7.5, 292 mM sucrose, 1 mM PMSF, 0.5 mM DTT, 1 μg/ml leupeptin), and transferred to a small beaker fitted with a magnetic stirrer bar. NaCl was added dropwise to a final concentration of 150 mM, and extraction continued for 1 h at 4 °C. The nuclei were pelleted by centrifugation at 14,500 × *g* for 20 min at 4 °C in a tabletop centrifuge. The supernatant was transferred and dialyzed 2 × 1 h at 4 °C against 1 liter of cold dialysis buffer (25 mM HEPES-KOH, pH 7.5, 50 mM KCl, 0.1 mM EDTA, 231 mM sucrose, 1 mM PMSF, 2 mM DTT, 1 μg/ml leupeptin). The dialyzed extract was clarified by centrifugation at 20,000 × *g* for 15 min at 4 °C. The supernatant was aliquoted, snap frozen in liquid nitrogen, and stored at −80 °C. The protein concentration was determined with the Bradford assay, and the salt concentration was measured using a conductivity meter.

X. laevis Egg Extracts

S phase extract was prepared as described previously (29). Briefly, eggs were dejellied, activated with calcium ionophore (Sigma-Aldrich), rinsed with S buffer (50 mM HEPES-KOH, pH 7.5, 50 mM KCl, 2.5 mM $MgCl_2$, 250 mM sucrose), transferred to 2-ml Eppendorf tubes, and crushed by centrifugation for 12 min at 13,200 rpm. The cytoplasmic layer was removed and after addition of CytB (Sigma-Aldrich) cleared by centrifugation for 25 min at 70,000 rpm (Sorvall TL55 swinging bucket rotor). The extract was supplemented with 250 μg/μl cycloheximide, 25 mM phosphocreatine, and 10 μg/ml creatine phosphokinase before use.

Western Blotting and Antibodies

Whole cell extracts of the cell lines were prepared using 2× Laemmli buffer (120 mM Tris-HCl, pH 6.8, 4% SDS, 20% glycerol). Upon determination of the protein concentration by the Lowry assay, proteins were separated by SDS-PAGE. Western blot analyses were carried out using standard procedures. The following antibodies and dilutions were used: MYH (mouse monoclonal, Abcam, ab55551), 1:333; OGG1 (rabbit monoclonal, Abcam, ab124741),1:10,000; MSH6 (mouse monoclonal, BD Transduction Laboratories, 610919), 1:1000; MSH2 (mouse monoclonal, Calbiochem, NA-27), 1:500; MLH1 (mouse monoclonal, BD Transduction Laboratories, 554073), 1:500; and TF II H (rabbit polyclonal, Santa Cruz Biotechnology, sc-293), 1:1000. The anti-MTH1 antibody was a generous gift from Yusaku Nakabeppu and was used at a dilution of 1:250. Horseradish peroxidase (HRP)-coupled anti-mouse and anti-rabbit secondary antibodies (GE Healthcare) were used at a dilution of 1:5000.

Substrate Generation

The detailed procedure was described previously (30). Briefly, hetero- and homoduplexes were constructed by primer extension on single-stranded phagemid templates. The templates differed in the position of the Nt.BstNBI site, which was situated at nucleotide 2850 either in the viral (top) or complementary (bottom) strand. Incubation of the substrates with the nickase yielded substrates in which MMR occurred either 5′ to 3′ or 3′ to 5′, respectively. The mismatches were located within a SalI and/or AclI restriction site, which was restored upon repair. The desired closed-circular heteroduplex substrates were purified on cesium chloride gradients.

Primers

The G^O- or A^O-containing primers were obtained from Eurogentec (Seraing, Belgium). All other primers were obtained from Microsynth (Balgach, Switzerland). The SalI (GTCGAC) and AclI (AACGTT) restriction sites are highlighted in bold and gray, respectively. PvuI restriction sites (CGATCG) are italicized, and mispaired residues are underlined. Primer sequences correspond to the outer strand sequence of the substrate. The substrates and the primer/template combinations are listed in Table 1.

Prenicking of Substrates

MYH + APE1—200 ng of the substrates were incubated with 10 ng of purified recombinant MYH-GST and 10 units of APE1 (New England Biolabs) in 1× MMR buffer (20 mM Tris-HCl, pH 7.6, 40 mM KCl, 5 mM $MgCl_2$, 1 mM glutathione, 50 μg/ml BSA, 0.1 mM dNTPs) for 4 h at 37 °C. The reaction was stopped by heat inactivation, and 50 ng of the prenicked substrate were analyzed on a 1% GelRed-stained agarose gel for nicking efficiency. The remaining 100 ng of the prenicked substrate were used in a MMR assay.

OGG1—1 μg of G^O/C-G/T substrate was incubated with 0.8 μg of purified recombinant OGG1 in 20 mM Tris-HCl, pH 8, 1 mM DTT, 1 mM EDTA, and 0.1 mg/ml BSA for 2.5 h at 37 °C and subsequently purified on a MinElute Spin column (Qiagen). 100 ng of the prenicked substrate were used in a MMR assay.

Nt.BstNBI—Closed-circular DNA substrates (100 ng) were incubated with 1 unit of Nt.BstNBI (New England Biolabs) according to the recommendations of the manufacturer. Subsequently, they were purified on a MinElute Spin column and used in MMR assays.

In Vitro MYH Nicking Assay

100 ng of closed-circular G^O/A, A^O/G, A^O/C, or homoduplex substrate were incubated with 10 ng of purified recombinant MYH-GST, 10 units of APE1, and 1.5 mM ATP in 1× MMR buffer in a total volume of 10 μl. For time course experiments, 5-μl aliquots were withdrawn at the indicated time points. The reactions were stopped by the addition of 2 μl of 6× loading dye (37.5 mg/ml Ficoll 400, 23% glycerol, 0.03% bromphenol blue) and subsequent heat inactivation. The samples were separated on 1% agarose gels and visualized with GelRed. The nicking efficiency was quantified from the ratio of the amount of open-circular DNA product to the total amount of DNA (closed-circular + open-circular).

In Vitro MMR Assay in Nuclear Extracts of Human Cells

The MMR assays were described previously (7, 30, 31). Unless otherwise specified, the reactions were carried out with 100 ng of substrate and 100 μg of nuclear cell extract in a total volume of 25 μl in a buffer containing 20 mM Tris-HCl, pH 7.6, 5 mM $MgCl_2$, 1 mM glutathione, 50 μg/ml BSA, 0.1 mM dNTPs, 1.5 mM ATP, and 80 mM KCl (in experiments involving MYH-addressed substrates) or 110 mM KCl (in experiments involving OGG1-addressed substrates). 1.8 pmol of purified MutLα or MutSα were added where indicated. The reactions were incubated at 37 °C for 1 h. The reaction was stopped by adding an equal volume of STOP solution (50% Proteinase K, 1 mM EDTA, 3% SDS) and subsequent incubation for 1 h at 50 °C. Substrates were purified on MinElute spin columns and subjected to SalI/DraI or AclI restriction digestion, and the DNA fragments were separated on 1% agarose gels stained with GelRed. The percentage of mismatch repair was quantified from the ratio of the repaired bands (c + d) to the total amount of DNA (c + d + (c + d)) using ImageQuantTL. The band intensities were corrected according to their respective DNA fragment sizes. Some assays were supplemented with 2 μCi of [α-^{32}P]dATP. To monitor incorporation of the radiolabeled nucleotide, the agarose gels were vacuum-dried, exposed to a Phosphor Screen, and scanned with a Typhoon Scanner (FLA 9500, GE Healthcare).

In Vitro MMR Assay in X. laevis Egg Extracts

Briefly, the reaction mixture containing 150 ng of substrate, 26 μl of S phase extract, and 2 μCi of [α-^{32}P]dATP in a total volume of 30 μl was incubated at 23 °C for 45 min. To inhibit replication, 500 nM geminin and 40 μg/ml p27 were added. The reaction was stopped by the addition of 70 μl of STOP solution (76 mM EDTA, 1.5% SDS) and 40 μg of RNase (Sigma-Aldrich) and incubated for 30 min at 37 °C. Subsequently, 200 μg of Proteinase K (AppliChem) were added, and incubation continued at 37 °C overnight. The substrates were purified on MinElute Spin columns and subjected to SalI/DraI or AclI restriction digestion in the presence of RNase. The digested DNA was cleaned up again and analyzed on a 1% agarose gel stained with GelRed.

Immunodepletions

20 μl of Protein A/G PLUS-agarose beads (sc-2003, Santa Cruz Biotechnology) were washed twice with 750 μl of binding buffer (30 mM HEPES-KOH, pH 7.6, 7 mM $MgCl_2$) and spun down at 2700 × *g* for 2 min at 4 °C. The beads were resuspended in binding buffer, and 1 μg anti-MYH or anti-MSH6 antibody was added. The mixture was then incubated for 3 h at 4 °C, the beads were washed three times with 750 μl of binding buffer, and subsequently used to immunodeplete 100 μg of nuclear cell extracts for 30 min at 4 °C. MMR assays were performed immediately after depletion. Mock-depleted nuclear cell extracts were obtained by incubation with beads only.

MMR- and/or BER-dependent Incorporation Assays

This assay was used to test MMR or BER activities. It was performed similarly to the MMR assay except for the following modifications. To track MMR-, MYH-, or OGG1-dependent nucleotide incorporation, the reactions were supplemented with 2 μCi of [α-^{32}P]dATP, [α-^{32}P]dCTP, or [α-^{32}P]dGTP, respectively. Finally, the substrates were digested with NotI/BsaI and analyzed on a GelRed-stained 1% agarose gel. Repair tracts of up to 330 bp in Nt.BstNBI-nicked substrates, up to 29 bp in the G^O/A substrates, and up to 22 bp in the G^O/C substrates are seen in the 1808-bp fragment a. Longer repair tracts appear in the 1387-bp fragment b (see Fig. 1*A*). Although MMR-dependent [^{32}P]dAMP incorporation gave rise to a strong radioactive signal in both bands, MYH-dependent [^{32}P]dCMP or OGG1-dependent [^{32}P]dGMP incorporation occurred only in DNA fragment a. Quantification of [^{32}P]-dCMP or [^{32}P]dGMP incorporation in MYH- or OGG1-induced BER was determined from the ratio between the band intensities of fragment a on the autoradiographs and on the GelRed-stained agarose gels.

BER Assay

To determine A^O/G to C/G or A^O/C to G/C repair by MYH-dependent BER, the substrates were incubated with the extracts as described for the MMR assay. After the reaction, 50% of the purified, eluted substrate was digested with SalI/DraI (MMR

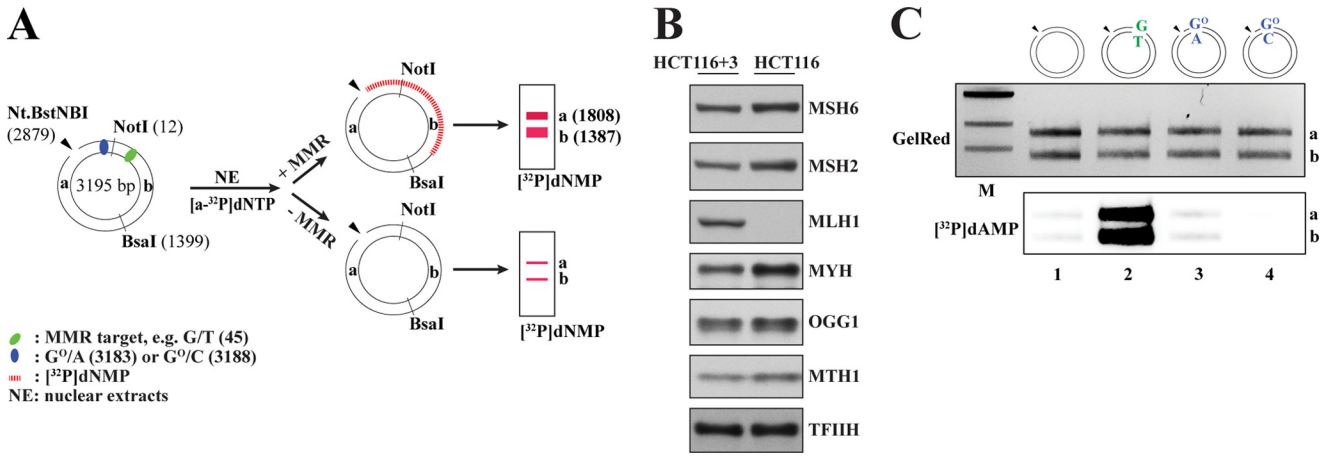

FIGURE 1. **G^O-containing mispairs are poor substrates for mismatch repair in human cell extracts.** *A*, schematic representation of the MMR-dependent nucleotide incorporation assay using 5′-nicked substrates. In the absence of an MMR target or in MMR-deficient extracts (−*MMR*), very little repair-mediated [^{32}P]dNMP incorporation takes place. In the presence of an MMR target in MMR-proficient extracts (+*MMR*), MMR-mediated [^{32}P]dNMP incorporation can be detected upon NotI/BsaI digestion of the phagemid DNA in both the 1808-bp fragment a and 1387-bp fragment b. Positions of the modified base pairs/mispairs in the plasmid are as follows: G^O/A, 3183; G^O/C, 3188; G/T, 45. *B*, Western blot analysis of HCT116 (MMR-deficient) and HCT116 + chromosome 3 (MMR-proficient) nuclear cell extracts to verify the presence and relative abundance of MMR (MSH6, MSH2, and MLH1) and BER (MYH, OGG1, and MTH1) proteins. The absence of MutLα in HCT116 cells is well documented (27). Where indicated, the extracts were complemented with the respective purified recombinant proteins during the MMR assays. *C*, G^O/A and G^O/C base pairs are not efficient substrates for MMR. 5′-Nicked substrates containing either no mismatch (*lane 1*), a G/T (*lane 2*) or G^O/A (*lane 3*) mismatch, or a G^O/C base pair (*lane 4*) 306–363 nucleotides away from the nick were incubated with HCT116 nuclear cell extracts supplemented with purified recombinant MutLα and [α-^{32}P]dATP. Upon NotI/BsaI restriction digestion, GelRed-stained DNA served as the DNA loading control, whereas the autoradiograph visualized MMR-dependent repair tracts in fragments a and b by means of [^{32}P]dAMP incorporation. *M*, molecular size marker (1-kb ladder; New England Biolabs).

assay), whereas the other half was used for PvuI digestion (BER assay).

RESULTS

G^O/A and G^O/C Mispairs Are Not Addressed by Canonical MMR—BER and MMR are mechanistically distinct biochemical pathways. They differ principally in their substrate specificity and in repair patch size. The specificity of BER is dictated by the enzymes that initiate the process, DNA glycosylases, which recognize and excise a limited number of damaged or modified bases (32). The repair process is thus initiated at the site of the base modification and involves the replacement of one (short patch BER) (33) or only 2–6 (long patch BER) nucleotides (34, 35). Canonical MMR addresses non-Watson-Crick base pairs that arise during replication, but in contrast to BER, the excision process initiates at a site distal to the mispair at a strand discontinuity that marks the nascent DNA strand. The repair tracts can thus be several hundred nucleotides long (36, 37). Because we wished to study the potential interplay of BER and MMR in the processing of substrates that could conceivably be addressed by both repair systems, we first needed to learn whether both repair pathways were active in our cell extracts and to establish experimental conditions that would allow us to differentiate between the two processes (Figs. 1*A*, 2*B*, and 5*F*). We first tested whether MMR was active in our cell extracts. To this end, we generated covalently closed circular phagemid substrates containing a single G/T, G^O/C, or G^O/A base pair or a control substrate containing a G/C at the same site. By subsequent nicking of the substrates at their Nt.Bst.NBI sites, we generated an initiation site for MMR (Fig. 1*A*). We then incubated the nicked substrates with extracts of MutLα-deficient HCT116 human cells (Fig. 1*B*) that were supplemented with purified recombinant MutLα and [α-^{32}P]dATP. Following recovery of the phagemids, restriction digestion with NotI and BsaI, and separation of the fragments on agarose gels, we anticipated that long patch repair events (MMR) would give rise to heteroduplexes labeled in both fragments a and b (Fig. 1*A*).

As shown in Fig. 1*C*, intense radiolabeling was seen only in the *bona fide* MMR substrate G/T (*lane 2*). That both fragments a and b were labeled with similar intensity indicates that the repair patch spanned at least the distance of 361 nucleotides between the nick and the mispair. Only background amounts of [^{32}P]dAMP were detected in fragments a and b of the control homoduplex, G^O/A, or G^O/C substrates (*lanes 1*, *3*, and *4*), which confirmed that the G^O/C and G^O/A pairs failed to activate nick-dependent long patch excision and resynthesis characteristic of MMR (38, 39) and exemplified in *lane 2*.

MYH-dependent BER in Human Nuclear Cell Extracts—Having shown that MMR was active in the extracts, but that it did not address the G^O/A and G^O/C substrates, we wanted to see whether they were processed by BER. G^O/A repair should be initiated by MYH, which should remove the mispaired adenine. The resulting apurinic site should then be incised by APE1. We therefore asked whether incubation of the supercoiled G^O/A substrate with purified, recombinant MYH-GST and APE1 gave rise to nicked circular molecules. As shown in Fig. 2*A* (*lanes 3–6*), the G^O/A substrate was efficiently converted to the open-circular form upon incubation of the plasmid with the recombinant proteins.

MYH has been reported to excise (in addition to adenine from mispairs with G^O) also the oxidation product of adenine, A^O, from mispairs with guanine or cytosine (23, 24). We therefore included the covalently closed A^O/G and A^O/C substrates in this assay. As shown in Fig. 2*A*, only limited nicking was detected on the A^O/G (*lanes 7–10*) and A^O/C (*lanes 11–14*)

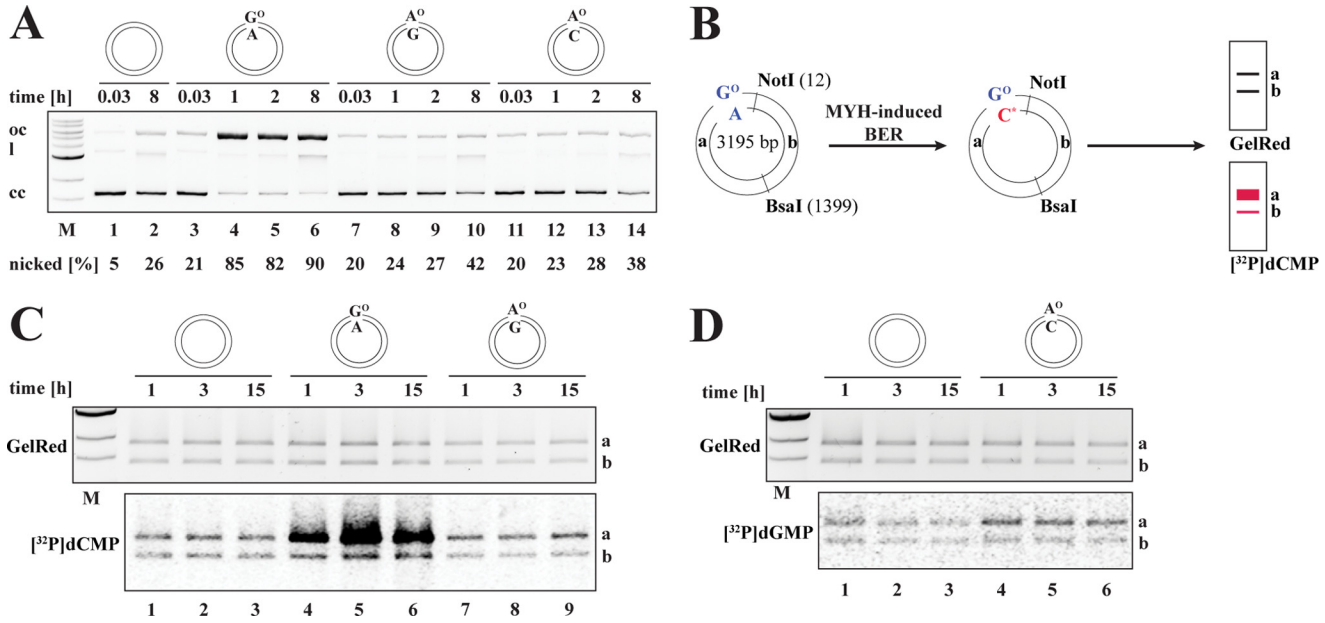

FIGURE 2. **MYH is active in HCT116 extracts and addresses G^O/A but not A^O/G or A^O/C mispairs.** *A*, nicking assay. The closed-circular homoduplex or the G^O/A, A^O/G, or A^O/C substrates were incubated with recombinant, purified MYH-GST and APE1 for the indicated times and analyzed by agarose gel electrophoresis. The mobility of the closed-circular (*cc*), open-circular (*oc*), and linear (*l*) DNA molecules is indicated on the *left*. The quantification shows the percentage of open-circular substrate compared with the total amount of DNA (open-circular + closed-circular). Only the G^O/A substrate was cleaved with appreciable efficiency. *B*, schematic representation of the MYH-dependent nucleotide incorporation assay. Short patch BER should replace the mispaired A with a radiolabeled C (*asterisk*). This should result in detectable radioactivity in band a of the NotI/BsaI digest. *C*, BER-dependent incorporation assay. The supercoiled homoduplex (*lanes 1–3*), G^O/A (*lanes 4–6*), and A^O/G (*lanes 7–9*) substrates were incubated with HCT116 extracts for the indicated time points. The reactions were supplemented with [α-^{32}P]dCTP. As visualized in the autoradiograph, [^{32}P]dCMP incorporation into fragment a of a NotI/BsaI-digested phagemid, indicative of short patch repair, was detected above background only in the G^O/A substrate. *D*, the supercoiled homoduplex (*lanes 1–3*) and A^O/C (*lanes 4–6*) substrates were incubated with the extracts for the indicated time points in reactions supplemented with [α-^{32}P]dGTP. Only low levels of radioactive nucleotide were incorporated into fragment a of a NotI/BsaI-digested A^O/C phagemid, indicative of inefficient BER. *M*, molecular size marker.

substrates with only 42 and 38% of the plasmids having been nicked after 8 h, respectively. This was only slightly above the nonspecific nicking levels observed on the homoduplex (26%).

We next set out to test BER activity in the extracts. MYH-initiated BER of G^O/A should give rise to G^O/C. Thus, upon incubation of the covalently closed G^O/A substrate with extracts supplemented with [α-^{32}P]dCTP, specific incorporation of [^{32}P]dCMP into fragment a of the substrate (Fig. 2*B*) should be detectable. This was indeed the case (Fig. 2*C*, *lanes 4–6*). As in the case of the purified enzymes, after incubation of the A^O/G (Fig. 2*C*, *lanes 7–9*) or A^O/C (Fig. 2*D*, *lanes 4–6*) substrate with [α-^{32}P]dCTP- or [α-^{32}P]dGTP-supplemented HCT116 extracts, respectively, the amount of radionucleotide incorporated into the A^O-containing fragment a of the two substrates was only slightly greater than that detected in the homoduplex substrate.

MYH-dependent Mismatch Repair in Human Nuclear Cell Extracts—Having obtained preliminary evidence that both MYH-dependent BER and MMR were active in the extracts, we next wanted to learn whether there was a cross-talk between these processes. To address this question, we deployed a phagemid substrate containing a G/T mismatch within the unique SalI restriction site (G/T; covalently closed or nicked with Nt.BstNBI 376 nucleotides 3′ from the mispaired T), a phagemid containing a single G^O/A mispair in addition to the G/T (G^O/A-G/T), and a control phagemid (G^O/A-G/C). Upon incubation with the cell extracts, the recovered phagemids were digested with SalI and DraI to give rise to the pattern of bands shown in Fig. 3*A*. Successful repair of the G/T mismatch to G/C regenerates the SalI site, and the plasmid is cut into four instead of three fragments (the smallest DraI fragment runs out of the gel and is therefore not seen). This process should be dependent on the presence of a nick in the strand containing the mispaired T as canonical MMR requires a strand discontinuity for initiation of the EXO1-dependent excision step (40, 41).

When the above substrates were incubated with MMR-deficient HCT116 nuclear cell extracts supplemented with [α-^{32}P]dATP, only background levels of repair and [^{32}P]dAMP incorporation were detected in the *bona fide* MMR substrate, nicked G/T (Fig. 3*B*, *lane 2*). However, the same substrate was repaired with high efficiency when the extracts were supplemented with purified recombinant MutLα (*lane 3*), particularly when compared with the unnicked control G/T plasmid (*lane 1*), which was processed to a limited extent by non-canonical MMR (42). Strikingly, although only low levels of [^{32}P]dAMP incorporation were detected in this system when the closed-circular G^O/A-G/C control substrate was used (*lanes 6* and *7*), around 60% of the covalently closed G^O/A-G/T phagemid were repaired in the extract supplemented with recombinant MutLα (*lane 5*). This result implied that A opposite G^O can serve as a cryptic strand discrimination signal for MMR.

We postulated that the MMR machinery might be hijacking intermediates of G^O/A processing for EXO1 loading. We therefore set out to confirm that the above described phenomenon was dependent on MYH by immunodepleting it from the extract (Fig. 3*C*) prior to incubation with the substrates. This reduced MMR efficiency on the G^O/A-G/T substrate from 52 (*lane 7*) to ~20% (*lane 8*). The latter level was comparable with

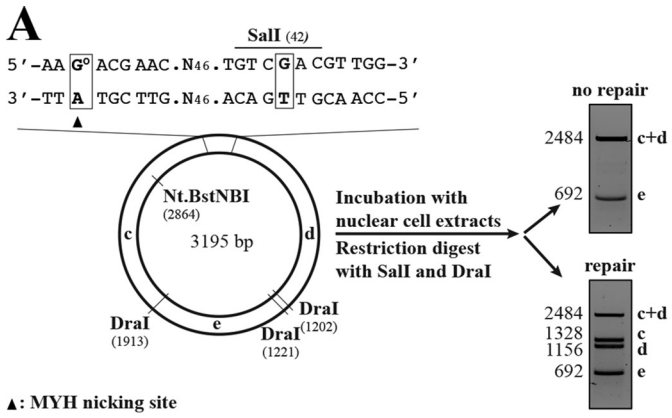
A
SalI (42)
5′-AA Gº ACG AAC . N46 . TGT C G A CGT TGG-3′
3′-TT A TGC TTG . N46 . ACA G T T GCA ACC-5′
Nt.BstNBI
(2864)
3195 bp
c
d
e
DraI
(1913)
DraI
(1221)
DraI(1202)
Incubation with
nuclear cell extracts
Restriction digest
with SalI and DraI
no repair
2484
692
c+d
e
repair
2484
1328
1156
692
c+d
c
d
e
▲: MYH nicking site

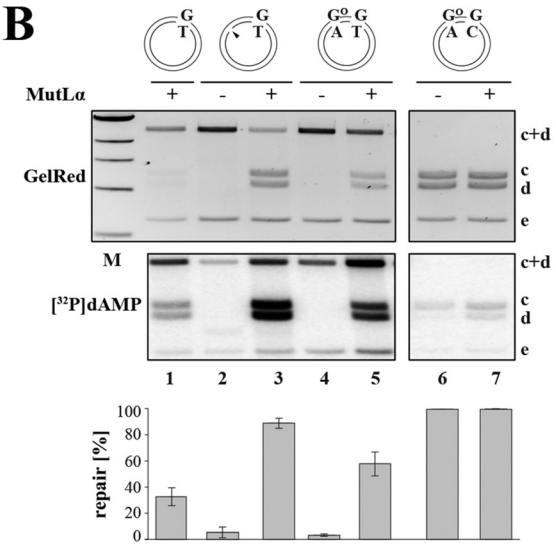
B
MutLα
GelRed
M
[32P]dAMP
c+d
c
d
e
1 2 3 4 5 6 7
repair [%]
100
80
60
40
20
0

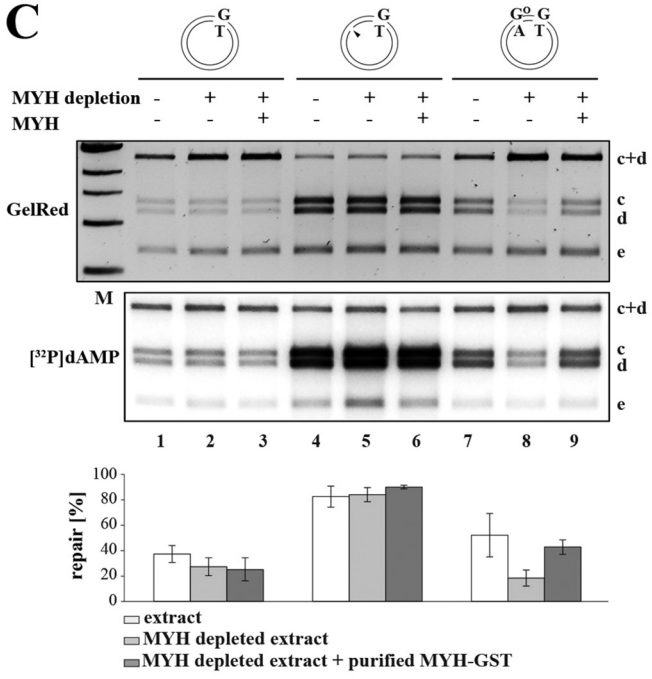
C
MYH depletion
MYH
GelRed
M
[32P]dAMP
c+d
c
d
e
1 2 3 4 5 6 7 8 9
repair [%]
100
80
60
40
20
0
extract
MYH depleted extract
MYH depleted extract + purified MYH-GST

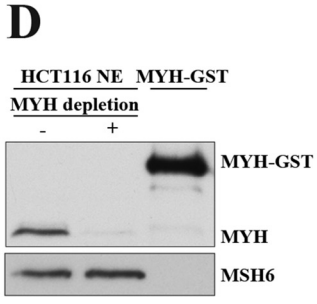
D
HCT116 NE
MYH-GST
MYH depletion
MYH-GST
MYH
MSH6

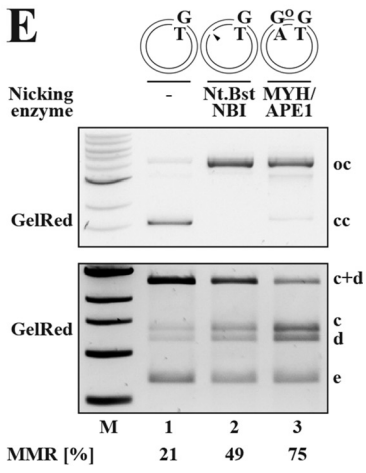
E
Nicking
enzyme
Nt.Bst
NBI
MYH/
APE1
GelRed
oc
cc
c+d
c
d
e
M 1 2 3
MMR [%] 21 49 75

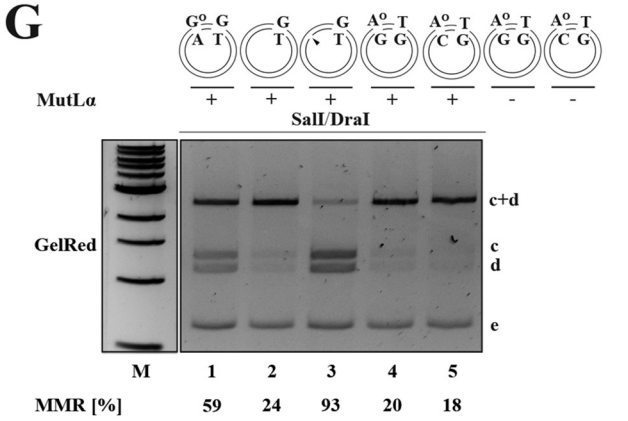
G
MutLα
SalI/DraI
GelRed
c+d
c
d
e
M 1 2 3 4 5
MMR [%] 59 24 93 20 18

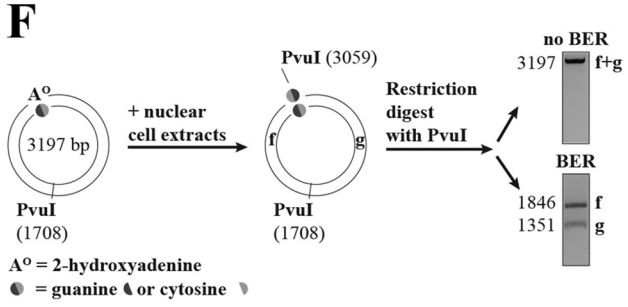
F
Aº
3197 bp
PvuI
(1708)
+ nuclear
cell extracts
PvuI (3059)
f
g
PvuI
(1708)
Restriction
digest
with PvuI
no BER
3197
f+g
BER
1846
1351
f
g
Aº = 2-hydroxyadenine
= guanine or cytosine

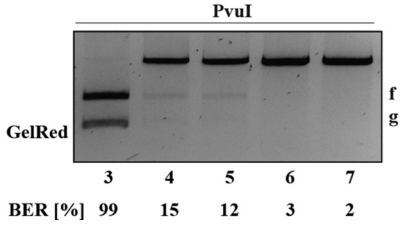
PvuI
GelRed
f
g
3 4 5 6 7
BER [%] 99 15 12 3 2

the efficiency of non-canonical MMR on the covalently closed G/T substrates (~30%) (*lanes 1–3*). That the observed inhibition was due to MYH depletion was confirmed by complementation of the depleted extracts with purified, recombinant MYH-GST (Fig. 3*D*), which restored the MMR efficiency on the G^O/A-G/T substrate to 43% (Fig. 3*C*, *lane 9*). As anticipated, MMR efficiencies on the G/T (*lanes 1–3*) and nicked G/T (*lanes 4–6*) substrates were unaffected by the amount of MYH-GST in the extracts.

To confirm that processing of G^O/A intermediates by the BER machinery indeed generates DNA termini that can be utilized by EXO1 in the strand degradation step of MMR, we preincubated the closed-circular G^O/A-G/T substrate with purified, recombinant MYH-GST and APE1 (Fig. 3*E*, *upper panel*, *lane 3*), which cleaves the sugar-phosphate backbone at the MYH-generated abasic site. We then incubated the MYH/APE1-nicked substrate with HCT116 extracts supplemented with MutLα. As shown in Fig. 3*E* (*lower panel*), the MYH/APE1-generated nick in the G^O/A-G/T substrate (*lane 3*) was efficiently recognized by MMR factors. That the latter substrate was even more efficiently repaired than the Nt.BstNBI-nicked G/T phagemid (*lane 2*) is most likely indicative of the shorter distance between the nick and the mispair in the G^O/A-G/T substrate (54 nucleotides) as compared with the Nt.BstNBI-nicked G/T phagemid (361 nucleotides).

We extended the *in vitro* MMR assays also to substrates containing an A^O/G or an A^O/C pair in the vicinity of a T/G mismatch. These substrates differed from those described above inasmuch as the A^O residues were located within a PvuI site (see "Experimental Procedures"). Successful repair of A^O/G to C/G or of A^O/C to G/C by BER would restore the restriction site such that PvuI digestion of the recovered DNA would allow quantification of BER activity at the A^O sites (Fig. 3*F*). As anticipated from the absence of detectable BER activity on these substrates, incubation of the A^O/G-T/G and A^O/C-T/G substrates with MMR-proficient HCT116 extracts supplemented with recombinant MutLα yielded only 15 and 12% PvuI-sensitive products, respectively (Fig. 3*G*, *lower panel*, *lanes 4* and *5*), whereas the G/T phagemid was completely digested under identical conditions (*lane 3*). These results were reflected in MMR efficiency determined from the same assays by digestion of the recovered phagemids with SalI/DraI (Fig. 3*G*, *upper panel*). Repair of the T/G mismatch in the A^O/G-T/G and A^O/C-T/G substrates was very inefficient (20 and 18%, respectively), whereas the nicked G/T (*lane 3*) and the covalently closed G^O/A-G/T (*lane 1*) substrates were efficiently repaired (93 and 59%, respectively). Taken together, these data show that A^O/G or A^O/C pairs are inefficiently processed by MYH in cell extracts and therefore fail to act as entry sites for mismatch-activated excision.

G^O/A Mispairs Act as MMR Initiation Sites also in X. laevis Egg Extracts—Because G^O/A mispairs arise during replication, MYH should be able to act on newly replicated DNA, and indeed, available experimental evidence shows that this glycosylase is more abundant during S phase (43). In an attempt to learn whether MYH is also more efficient during S phase, we decided to make use of *X. laevis* egg extracts, which are enriched in S phase proteins (44).

In the first experiment, we wanted to learn whether the extracts were proficient in MYH-initiated BER. We decided to make use of the assay described above (Fig. 2*B*) in which the homoduplex or G^O/A closed-circular substrates were incubated with *X. laevis* egg extracts supplemented with [α-^{32}P]dCTP. Digestion of the recovered phagemid DNA with NotI/BsaI revealed a 3-fold greater incorporation of [^{32}P]dCMP into the G^O-containing fragment of the G^O/A substrate than into the corresponding fragment of the homoduplex phagemid (Fig. 4*A*). This demonstrated that MYH-dependent BER was active in the *X. laevis* extracts.

FIGURE 3. **A single G^O/A base pair in a DNA heteroduplex can act as an initiation site for MMR in human nuclear cell extracts.** *A*, schematic representation of the G^O/A-G/T substrate and the *in vitro* MMR assay. The substrate carries a G^O/A mispair 57 nucleotides away from a G/T mismatch, which is located in a SalI recognition site. The presence of the mismatch makes the phagemid refractory to cleavage with the enzyme such that incubation with SalI and DraI yields fragments c + d (2484 bp) and e (692 bp). (The third, 19-bp-long fragment is not detectable on 1% agarose gels stained with GelRed.) The presence of a nick in the inner strand, introduced either by Nt.BstNBI or through BER-catalyzed incision of the A strand results in a repair of the G/T mismatch to G/C in human nuclear cell extracts that regenerates the SalI site. Upon incubation with SalI and DraI, the repaired phagemid gives rise to fragments c (1328 bp), d (1156 bp), and e (692 bp). *B*, G^O/A mispairs serve as initiation sites for MMR. The MMR assay shows the efficiency of repair of a G/T mismatch in closed-circular G/T (*lane 1*), nicked G/T (*lanes 2* and *3*), closed-circular G^O/A-G/T (*lanes 4* and *5*), and closed-circular G^O/A-G/C (*lanes 6* and *7*) substrates that were incubated with nuclear extracts of MutLα-deficient HCT116 cells supplemented with purified MutLα (+) where indicated. The autoradiograph shows MMR-dependent [^{32}P]dAMP incorporation into the different substrate fragments. *C*, G/T repair in the G^O/A-G/T substrate is dependent on MYH. The closed-circular G/T (*lanes 1–3*), nicked G/T (*lanes 4–6*), and closed-circular G^O/A-G/T (*lanes 7–9*) substrates were incubated with MutLα-supplemented extracts of HCT116 cells, which were either mock-depleted (*lanes 1*, *4*, and *7*), MYH-depleted (*lanes 2*, *5*, and *8*), or MYH-depleted and supplemented with recombinant MYH-GST (*lanes 3*, *6*, and *9*). The efficiency of the repair reactions shown in *B* and *C* was estimated by ImageQuant from scans of GelRed-stained agarose gels. The indicated MMR efficiencies (%) represent an average of three independent experiments. *Error bars* represent S.D. *D*, Western blot showing MYH immunodepletion efficiency of HCT116 nuclear cell extracts and the amount of recombinant MYH-GST used to supplement the depleted extracts. *E*, MYH/APE1-generated DNA termini at G^O/A sites are recognized by MMR. *Upper panel*, G^O/A-G/T phagemid (*lane 3*) was incubated with purified recombinant MYH-GST and APE1 (*lane 3*), and the G/T substrate either closed-circular (*lane 1*) or prenicked with Nt.BstNBI (*lane 2*) was mock-incubated (*lanes 1* and *2*) under the same experimental conditions. *Lower panel*, the pretreated substrates were purified and incubated with HCT116 nuclear extracts supplemented with MutLα. Subsequently, they were digested with SalI/DraI, and repair efficiencies were analyzed on a GelRed-stained agarose gel and quantified. The G/T mispair in the MYH/APE1-pretreated G^O/A-G/T substrate was efficiently repaired. The panel shows a representative image of two independent experiments. *F*, schematic representation of a BER assay using phagemid substrates containing A^O mispaired with guanine or cytosine. The A^O residue is located within a PvuI restriction site, which makes the phagemid refractory to cleavage with this enzyme. A^O/G to C/G or A^O/C to G/C repair by BER restores the PvuI site. Incubation with the enzyme gives rise to 1846-bp fragment f and 1351-bp fragment g. Positions are as follows: A^O/G, 3060; A^O/C, 3057. *G*, A^O/G and A^O/C mispairs do not serve as MMR initiation sites. The indicated substrates were incubated with MMR-deficient HCT116 extracts supplemented (+) or not (−) with purified MutLα. *Upper panel*, the efficiency of G/T to G/C (*lanes 1–3*) or T/G to C/G (*lanes 4* and *5*) repair mediated by MMR was estimated by SalI/DraI restriction digestion of the following recovered substrates: closed-circular G^O/A-G/T (*lane 1*), closed-circular G/T (*lane 2*), nicked G/T (*lane 3*), closed-circular A^O/G-T/G (*lane 4*), and closed-circular A^O/C-T/G (*lane 5*). *Lower panel*, an aliquot of the recovered phagemids was digested with PvuI, which detects MYH-dependent BER of A^O to C in the A^O/G substrate or of A^O to G in the A^O/C substrate. The nicked G/T substrate (*lane 3*) served as the positive control for PvuI digestion. A^O/G-T/G and A^O/C-T/G substrates that were not incubated with the extracts (*lanes 6* and *7*) contain defective PvuI sites and thus served as negative controls. MMR and BER efficiencies (%) are indicated below the panels. *M*, molecular size marker.

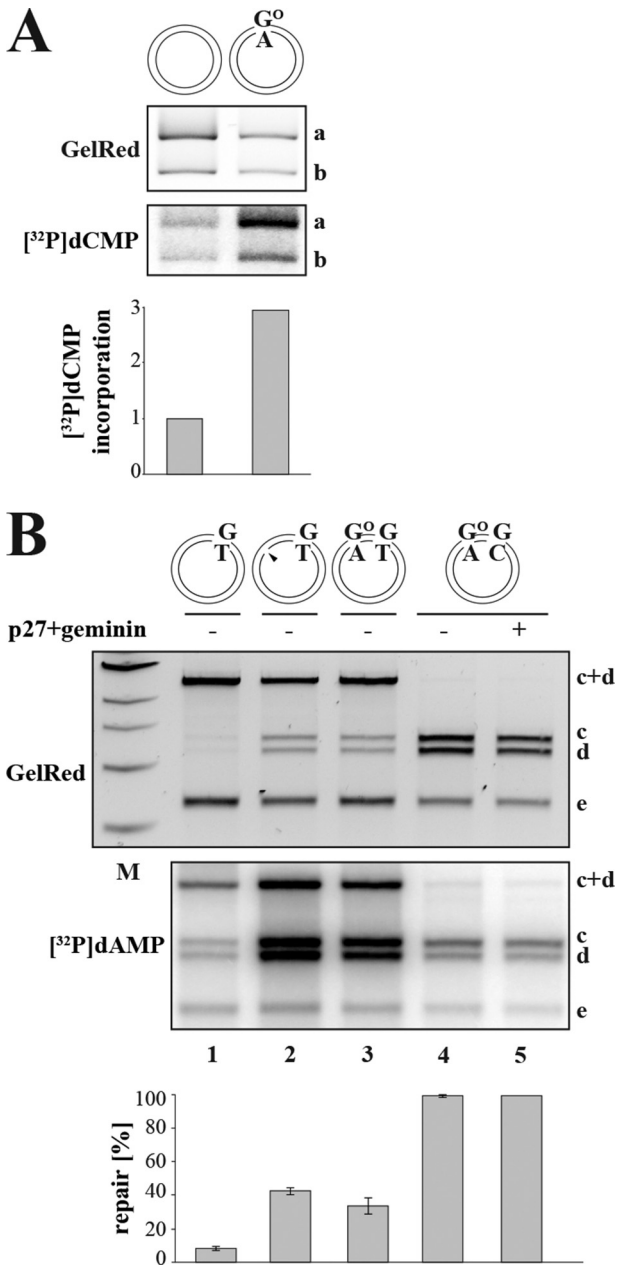

FIGURE 4. **Efficiency of MMR initiation at G^O/A sites in *X. laevis* egg extracts.** *A*, MYH is active in *X. laevis* eggs. Closed-circular homoduplex or G^O/A substrate was incubated with *X. laevis* egg extracts supplemented with [α-^{32}P]dCTP and subsequently digested with NotI/BsaI (see Fig. 1*A*). Although only background levels of [^{32}P]dCMP were incorporated into the homoduplex substrate (*lane 1*), substantial incorporation into the 1808-bp fragment a of the G^O/A substrate was detected (*lane 2*), which is indicative of base excision repair. For quantification, [^{32}P]dCMP incorporation into the homoduplex substrate was set to 1. The panel shows a representative image of two independent experiments. *B*, G^O/A serves as an initiation site for MMR in *X. laevis* egg extracts. G/T (*lane 1*), nicked G/T (*lane 2*), G^O/A-G/T (*lane 3*), or G^O/A-G/C (*lanes 4–5*) substrate was incubated with *X. laevis* egg extracts. Upon SalI/DraI digestion of the recovered phagemids, MMR efficiencies were estimated from the GelRed-stained agarose gels, whereas MMR-dependent DNA synthesis was visualized by [^{32}P]dAMP incorporation seen in the autoradiograph. A control reaction (*lane 5*) contained the replication inhibitors p27 and geminin; because [^{32}P]dAMP incorporation was similar in the presence and absence of these inhibitors (*cf. lanes 4* and *5*), the plasmid was apparently not replicated in the extracts (52). The indicated MMR efficiencies (%) represent an average of three independent experiments. *Error bars* represent S.D. *M*, molecular size marker.

We also had to show that the extracts supported nick-directed MMR because an earlier report indicated that mismatch processing in *X. laevis* oocyte extracts was efficient but not nick-directed (45). We therefore incubated the covalently closed and the nicked isoforms of the G/T phagemid with the extracts supplemented with [α-^{32}P]dATP. As shown in Fig. 4*B*, we were able to detect nick-directed MMR on the G/T substrate (*lane 2*), whereas the covalently closed phagemid was only inefficiently processed (*lane 1*). Under these conditions, the covalently closed G^O/A-G/T substrate (*lane 3*) was almost as efficiently repaired as the nicked G/T phagemid (*lane 2*). Because extracts of *X. laevis* eggs support plasmid replication under certain conditions, which would result in considerable [^{32}P]dAMP incorporation and conversion of 50% of the G/T mismatches to G/C in the absence of MMR, we carried out a control experiment in extracts supplemented with the DNA replication inhibitors p27 and geminin. No detectable differences between the levels of radionucleotide incorporation in the presence and absence of these inhibitors were observed, indicating that the plasmid did not replicate in the assay (*cf. lanes 4* and *5*).

OGG1-dependent Mismatch Repair Is Inefficient in Human Nuclear Cell and X. laevis Egg Extracts—Assuming that MTH1 hydrolyzes oxidized dGTP in the nucleotide precursor pool with a 100% efficiency, all G^O residues in oxidized DNA should be in the template strand following replication irrespective of whether they are paired with A or C. As discussed above, MYH-initiated BER of G^O/A mispairs arising during replication would be directed to the A strand that is also the nascent DNA strand. In contrast, BER-mediated repair of G^O/C pairs arising during replication would have the opposite effect on MMR because OGG1-dependent G^O/C repair would introduce breaks in the template DNA strand and thus provide MMR with an incorrect strand bias.

We set out to test the above hypothesis by studying the effect on MMR efficiency and directionality of a G^O/C pair situated in the vicinity of a G/T mismatch. We generated a G^O/C-G/T substrate in which the G^O was positioned 54 nucleotides 5′ from the mispaired G. OGG1-initiated BER of the G^O would give rise to a break that should activate MMR to correct the G/T mismatch to A/T and thus regenerate an AclI site in the substrate. This repair bias should be identical to that introduced by a Nt.Bst.NBI-generated nick in the G/T substrate (Fig. 5*A*).

When we incubated the nicked G/T substrate or the covalently closed G/T, G^O/C-G/T, or G^O/C-A/T phagemid heteroduplexes with HCT116 nuclear cell extracts supplemented with [α-^{32}P]dATP, no significant repair or [^{32}P]dAMP incorporation was observed (Fig. 5*B*, *lanes 1*, *3*, *5*, and *7*), but when the extract was supplemented with purified, recombinant MutLα, the Nt.BstNBI-nicked G/T substrate was repaired (*lane 4*). In contrast to what was observed with the G^O/A-G/T substrate (Fig. 3*B*, *lane 5*), only background levels of repair and [^{32}P]dAMP incorporation were detected with the G^O/C-G/T substrate (Fig. 5*B*, *lane 6*) and with the control, covalently closed G/T phagemid (*lane 2*). Similar results were obtained also with MutSα-deficient LoVo extracts supplemented with purified recombinant MutSα (Fig. 5*C*, *lanes 1–3*). Given that both extracts contained the key MMR and BER factors as ascer-

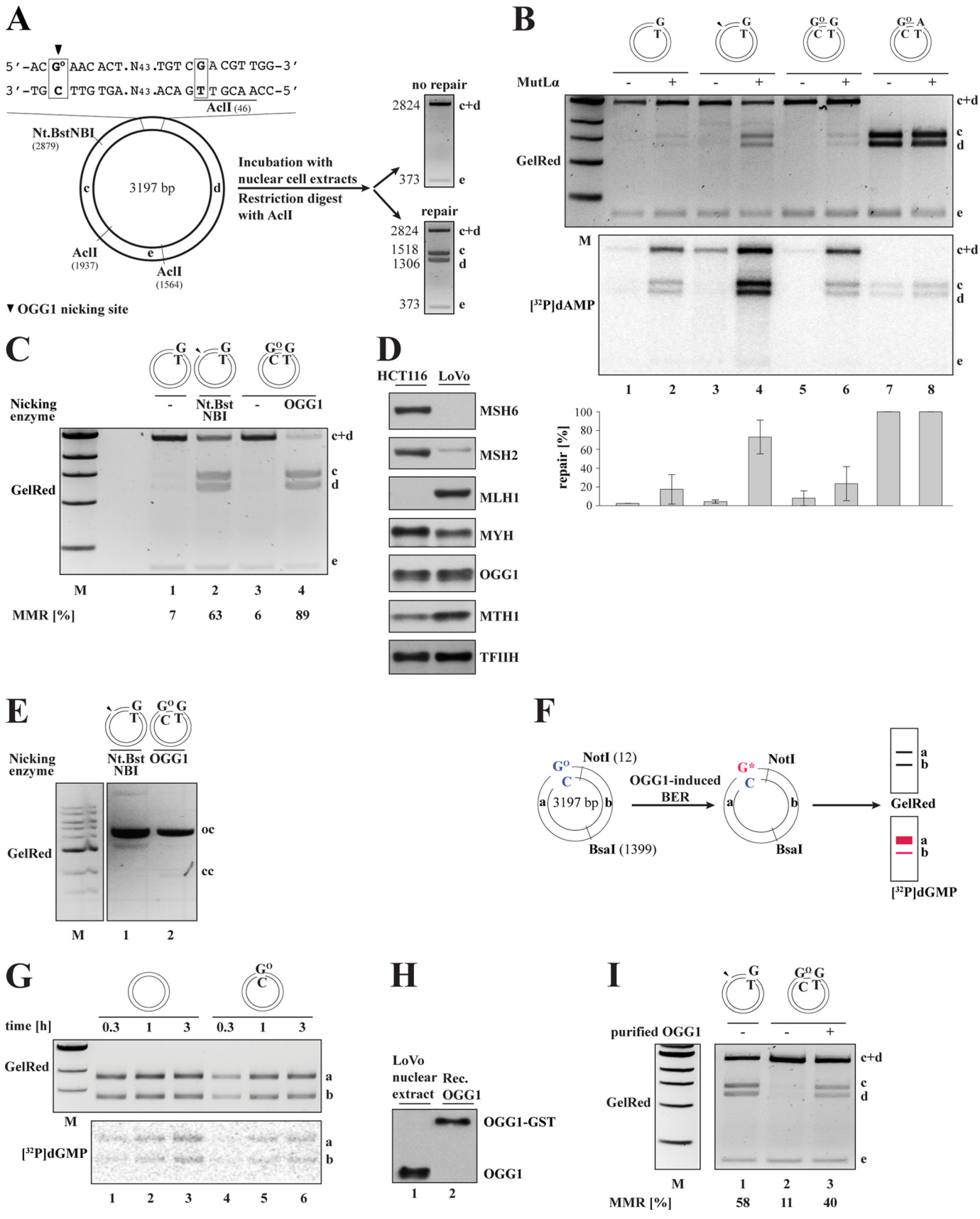
A
5′-AC Gº AAC ACT. N43 .TGT C G A CGT TGG-3′
3′-TG C TTG TGA. N43 .ACA G T T GCA ACC-5′
AclI (46)
Nt.BstNBI (2879)
3197 bp
c
d
e
AclI (1937)
AclI (1564)
▼ OGG1 nicking site
Incubation with nuclear cell extracts
Restriction digest with AclI
no repair
2824 c+d
373 e
repair
2824 c+d
1518 c
1306 d
373 e
B
MutLα
GelRed
M
[32P]dAMP
c+d
c
d
e
1 2 3 4 5 6 7 8
repair [%]
100 80 60 40 20 0
C
Nicking enzyme
Nt.Bst NBI
OGG1
GelRed
c+d
c
d
e
M 1 2 3 4
MMR [%] 7 63 6 89
D
HCT116 LoVo
MSH6
MSH2
MLH1
MYH
OGG1
MTH1
TFIIH
E
Nicking enzyme
Nt.Bst NBI
OGG1
GelRed
oc
cc
M 1 2
F
NotI (12)
OGG1-induced BER
NotI
BsaI (1399)
BsaI
GelRed
[32P]dGMP
a
b
G
time [h]
0.3 1 3 0.3 1 3
GelRed
M
[32P]dGMP
a
b
1 2 3 4 5 6
H
LoVo nuclear extract
Rec. OGG1
OGG1-GST
OGG1
1 2
I
purified OGG1
GelRed
c+d
c
d
e
M 1 2 3
MMR [%] 58 11 40

tained by Western blotting (Figs. 1*B* and 5*D*), these results at first suggested that G^O processing failed to activate MMR on the G^O/C-G/T substrate.

The above result could be explained in several ways. We first considered the possibility that the MMR machinery was unable to use the BER intermediates generated during G^O processing as strand discrimination signals because OGG1 is a DNA glycosylase/lyase that generates a strand break on the 3′ side of the abasic site (46, 47). APE1-mediated cleavage at its 5′ side then generates a single nucleotide gap rather than just a break at the 5′ side of the abasic site as is the case for MYH/APE1. We therefore treated the covalently closed G^O/C-G/T substrate with purified recombinant OGG1-GST fusion protein. As shown in Fig. 5*E* (*lane 2*), the substrate was as efficiently nicked as the G/T control with Nt.BstNBI (*lane 1*). When the OGG1-nicked phagemid was incubated with extracts of LoVo cells supplemented with purified recombinant MutSα, it was repaired with efficiency similar to that of the control, nicked G/T phagemid (Fig. 5*C*, *cf. lanes 2* and *4*). This shows that MMR can use OGG1-generated strand breaks as initiation sites.

The second possibility was that OGG1 in the tested cell extracts was inactive or that it was present in insufficient amounts. We therefore incubated the G^O/C and homoduplex substrates with LoVo extracts supplemented with [α-^{32}P]dGTP to test for OGG1-dependent BER, which should result in [^{32}P]dGMP incorporation into fragment a (Fig. 5*F*). As shown in Fig. 5*G*, only background levels of the radiolabeled nucleotide were incorporated into fragment a of the phagemid heteroduplex, suggesting that G^O/C repair was indeed inefficient despite the fact that the extracts contained readily detectable amounts of OGG1 (Figs. 1*B* and 5*D*). Similar results were obtained with ^{32}P-labeled G^O/C-containing oligomers, which were inefficiently processed in LoVo extracts, whereas processing of U/G-containing oligomers was very efficient. Moreover, purified, recombinant OGG1 was able to process the G^O/C oligonucleotide substrate with ~50% cleavage of the G^O strand seen after only 10 min (data not shown).

To test whether the LoVo extracts contained an inhibitor of OGG1, we supplemented them with an amount of purified recombinant OGG1-GST that was comparable with that of the endogenous protein present in the nuclear extracts (Fig. 5*H*). Under these conditions, the G^O/C-G/T substrate (Fig. 5*I*, *lane 3*) was repaired with efficiency similar to that of the nicked G/T phagemid (*lane 1*).

Importantly, the above described phenomenon was not limited to extracts of human cells as identical results were obtained with the *X. laevis* MMR system (Fig. 6). The reason underlying the low OGG1 activity in the extracts is currently unknown, but we were able to eliminate inappropriate salt concentration, lack of an activator protein in the cytoplasmic fraction, and short half-life of OGG1 in our assay as possible causes (data not shown).

DISCUSSION

The postreplicative mismatch repair system improves the fidelity of DNA replication by several orders of magnitude through removing from nascent DNA nucleotides that fail to form Watson-Crick base pairs. To fulfill this function, it has to satisfy two key criteria: it has to (i) recognize base-base mismatches and small insertion/deletion loops generated by the replicative polymerases during DNA synthesis and (ii) direct the repair process to the newly synthesized DNA strand. How the major mismatch recognition factor MutSα recognizes the different helical distortions that are caused by purine/purine, purine/pyrimidine, and pyrimidine/pyrimidine mispairs as well as by insertion/deletion loops is still poorly understood despite the fact that several structures of protein-DNA complexes exist (48). However, because MMR deficiency leads to transition, transversion, and frameshift mutations, MutSα clearly has broad substrate specificity. Although this characteristic of MutSα is beneficial as far as its role in the maintenance of replication fidelity is concerned, it might also be deleterious should MutSα bind to lesions that ought to be processed by other repair systems. One such example is mispairs containing

FIGURE 5. **A G^O/C base pair does not act as an initiation site for MMR in nuclear extracts of human cells.** *A*, schematic representation of the G^O/C-G/T substrate used in the *in vitro* MMR assay. The circular heteroduplex substrate carries a G^O/C base pair 54 nucleotides from a G/T mismatch in the recognition site of AclI endonuclease. The positions of two further AclI cleavage sites and the Nt.BstNBI site where a nick can be introduced selectively into the outer strand are indicated. In the absence of repair, digestion of the phagemid with AclI gives rise to fragments of 2824 (fragments c + d) and 373 bp (fragment e). Repair of the G/T mismatch to A/T regenerates a third AclI restriction site such that the phagemid DNA is cleaved into three fragments of 1518 (fragment c), 1306 (fragment d), and 373 bp (fragment e). *B*, substrates G/T (*lanes 1* and *2*), nicked G/T (*lanes 3* and *4*), G^O/C-G/T (*lanes 5* and *6*), and G^O/C-A/T (*lanes 7* and *8*) were incubated with extracts of HCT116 cells supplemented (+) or not (−) with purified recombinant MutLα and analyzed on a GelRed-stained agarose gel. The autoradiograph visualizes [^{32}P]dAMP incorporation into the different substrate fragments. The indicated MMR efficiencies (%) were estimated by ImageQuant from scans of GelRed-stained agarose gels and represent an average of three independent experiments. *Error bars* represent S.D. Only background levels of repair were detected in the G^O/C-G/T substrate (*lane 6*). *C*, OGG1-generated DNA termini at G^O/C sites act as MMR initiation sites. The G/T phagemid substrate was preincubated with Nt.BstNBI (*lane 2*), and the G^O/C-G/T phagemid was preincubated with recombinant, purified OGG1 (*lane 4*) to generate nicked, open-circular substrates (see *E*). The substrates were then purified and incubated with LoVo nuclear cell extracts supplemented with purified MutSα (*lanes 1–4*). The closed-circular G/T (*lane 1*) and G^O/C-G/T (*lane 3*) phagemid substrates served as controls. The OGG1 prenicked G^O/C-G/T substrate (*lane 4*) was at least as efficiently repaired as the positive control, nicked G/T (*lane 2*). *D*, Western blot analysis of the relative abundance of MMR (MSH6, MSH2, and MLH1) and BER (MYH, OGG1, and MTH1) proteins in nuclear extracts of HCT116 and LoVo cells. The absence of MutLα in HCT116 cells and of MutSα in LoVo cells is evident. Where required, these extracts were complemented with the purified recombinant proteins. *E*, the G^O/C-G/T phagemid substrate was preincubated with purified recombinant OGG1 (*lane 2*) to give rise to an open-circular (*oc*) substrate, which migrates in the 1% agarose gel in the same position as the Nt.BstNBI-nicked G/T substrate (*lane 1*). These prenicked substrates were purified and used in the MMR assay shown in *C*. *F*, schematic representation of the OGG1-dependent nucleotide incorporation assay. Short patch BER should replace the oxidized G with a radiolabeled G (*asterisk*). This should result in detectable radioactivity in band a of the NotI/BsaI digest. *G*, absence of OGG1 activity in human nuclear cell extracts. *Upper panel*, homoduplex (*lanes 1–3*) or G^O/C (*lanes 4–6*) substrate was incubated with LoVo extracts supplemented with [α-^{32}P]dGTP for the indicated times. As seen in the autoradiograph, both substrates incorporated similar amounts of [^{32}P]dGMP that were close to background. *H*, Western blot showing the amount of OGG1 in 100 μg of LoVo nuclear extract used in one MMR reaction (*lane 1*) and the amount of recombinant purified OGG1-GST required to supplement the reaction (*lane 2*). *I*, a G^O/C base pair activates MMR in LoVo extracts supplemented with purified, recombinant OGG1-GST. The nicked G/T (*lane 1*) and the G^O/C-G/T (*lanes 2–3*) substrates were incubated with LoVo nuclear cell extracts and purified MutSα supplemented (+) or not (−) with an amount of purified recombinant (*Rec.*) OGG1-GST shown in *H*, *lane 2*. *H* and *I* show representative images and quantifications of three independent experiments. *M*, molecular size marker.

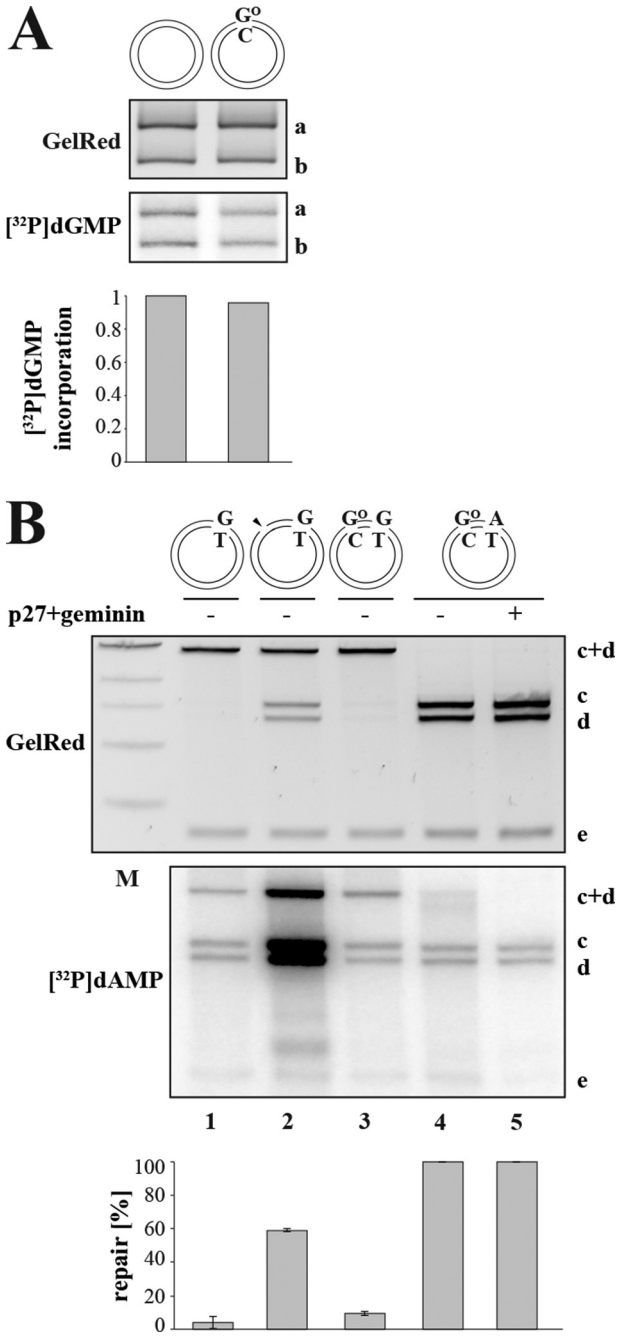

FIGURE 6. **A G^O/C base pair does not act as an initiation site for MMR in *X. laevis* egg extracts.** *A*, BER-dependent incorporation assay. *X. laevis* egg extracts lack OGG1 activity as only background levels of [^{32}P]dGMP were incorporated into fragment a of the control homoduplex (*lane 1*) and the G^O/C (*lane 2*) substrates. OGG1-dependent BER efficiencies were quantified from the intensity ratio between band a in the autoradiograph and the GelRed-stained agarose gel using ImageQuant. The panel shows a representative image of two independent experiments. *B*, the MMR activity in *X. laevis* egg extracts was determined using closed-circular G/T (*lane 1*), nicked G/T (*lanes 2*), G^O/C-G/T (*lane 3*), and G^O/C-A/T (*lanes 4* and *5*) substrates. That similar background levels of [^{32}P]dAMP were incorporated into the control G^O/C-A/T substrate in the absence (*lane 4*) and presence (*lane 5*) of the replication inhibitors p27 and geminin demonstrates that the phagemids were not replicated under these conditions (52). The panel shows a representative image of three independent experiments. Their average quantitation is shown below. *Error bars* represent S.D. *M*, molecular size marker.

O^6-methylguanine; these lesions activate MMR, but because their processing does not lead to the removal of the modified nucleotide from the template strand, they trigger futile repair that eventually leads to cell death (1). Processing of G^O/A mismatches arising through the incorporation of dAMP opposite G^O in the template strand might have also been expected to trigger futile MMR, but the *in vivo* evidence for such a process is currently lacking, and *in vitro* data showing that G^O/A mispairs are very poorly addressed by the MMR system in human cell extracts (this study and Ref. 39) would appear to argue against it. However, *in vivo*, the MMR system appears to remove from the nascent strand G^O misincorporated opposite template A (49, 50) and to increase the efficiency of MYH-dependent BER at least *in vitro* (51). Thus, available experimental evidence suggests that MMR supports BER during oxidative DNA damage processing. In the present study, we asked whether the reverse might also be true, namely whether BER-dependent processing of G^O affects MMR efficiency.

In our earlier studies, we showed that the MMR system could use breaks generated during the BER-mediated processing of uracil residues (7, 42) or during the RNase H2-mediated excision of ribonucleotides misincorporated into DNA during replication (9) as strand discrimination signals. We postulated that MMR might also use breaks generated during the BER-dependent processing of oxidative damage. However, the outcome of such interference would be positive only in the case that the breaks were generated in the nascent DNA strand. We show here that MYH-dependent processing of a G^O/A mispair in extracts of human cells or of *Xenopus laevis* eggs directs MMR to the A strand (Figs. 3 and 4). *In vivo*, the ability of the MMR system to use breaks generated during the MYH-directed processing of G^O/A mispairs arising through the incorporation of dAMP opposite G^O would direct mismatch correction to the nascent strand and thus improve the fidelity of replication (Fig. 7, *right panel*). MYH-dependent BER and MMR would thus synergize during S phase as might have been anticipated from the physical interaction of some of the subunits of these pathways (51). It could be argued that the number of G^O/A mispairs arising in the vicinity of a replication error might be too low to affect MMR efficiency. However, this number likely increases substantially when strand discontinuities arising during the processing of other "non-standard" nucleotides (uracils and thymines arising through deamination of cytosine and 5-methylcytosine, respectively; ribonucleotides; methylpurines; thymine glycols; etc.) are considered. Indeed, as we showed previously, ribonucleotide processing alone is sufficient to affect MMR efficiency *in vivo* (9).

Breaks introduced into the nascent DNA strand by OGG1 during the processing of C/G^O pairs arising through the incorporation of dG^OMP opposite template C would also help improve MMR efficiency and replication fidelity. However, due to the sanitization of dNTP pools by MTH1, dG^OTP concentrations should be extremely low such that dG^OMP incorporation into nascent DNA during replication should be minimal (Fig. 7, *left panel*). As a result, most G^O residues present in DNA during replication should be in the template strand. Incision of this strand by OGG1 behind the replication fork would misdirect MMR to the wrong strand (Fig. 7, *right panel*), and OGG1-catalyzed incision of DNA at G^O/C sites in front of the replication fork could cause its collapse. It would therefore appear logical that G^O/C processing should be completed prior to the

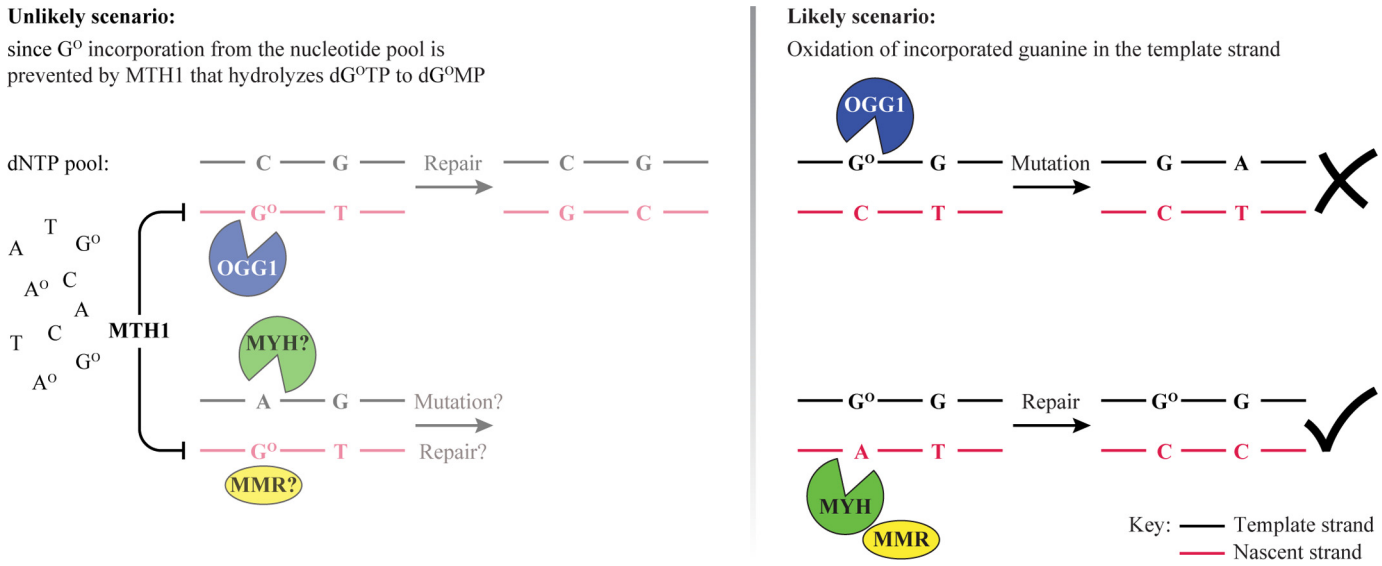

FIGURE 7. **Schematic representation of the BER and MMR interplay in G^O metabolism.** *Left panel*, should dG^OMP be incorporated into the nascent strand (*red*) opposite C, it could be removed by OGG1-dependent BER or by MMR without deleterious consequences. In contrast, should $A_{template}/G^O_{nascent}$ mispairs arise during replication, MYH-mediated BER to C/G^O would give rise to A to C mutations, whereas MMR would process the G^O-containing strand and prevent mutagenesis. In cases where the oxidized base was in the vicinity of a replication error (*e.g.* a G/T mispair), BER intermediates of $C_{template}/G^O_{nascent}$ processing would direct MMR to the correct strand, whereas MYH-initiated BER of $A_{template}/G^O_{nascent}$ would misdirect MMR to the parental template strand (*black*). However, the likelihood of incorporation of dG^OMP into the nascent DNA strand is minimized by hydrolysis of dG^OTP in the nucleotide pool by MTH1. Most G^O residues in the DNA should therefore be in the template strand as shown in the *right panel*. *Right panel*, BER of G^O/C pairs would lead to the removal of the oxidized base, but during S phase, the OGG1-generated strand break might result in replication fork collapse or in the misdirection of MMR to the template strand. Processing of $G^O_{template}/A_{nascent}$ mispairs by MYH-dependent BER or by MMR would have no deleterious consequences. Moreover, in cases where the oxidized base was in the vicinity of a replication error (*e.g.* a G/T mispair), BER intermediates of $G^O_{template}/A_{nascent}$ processing would direct MMR to the correct strand.

onset of S phase and that OGG1 should be inactivated during this cell cycle stage. Interestingly, we found that G^O/C processing in both *in vitro* systems was inefficient and that the presence of a G^O/C pair in the heteroduplex substrate failed to activate MMR of the G/T mismatch (Figs. 5 and 6) despite the fact that OGG1 was present in considerable quantities (Figs. 1*B* and 5, *D* and *H*). Because addition of the recombinant polypeptide to the extracts resulted in G^O-dependent G/T repair (Fig. 5*I*), we postulate that OGG1 present in the cell extracts is inactive either as a result of post-translational modifications or through complexation with an inhibitor. We are currently attempting to identify the underlying cause of this inhibition as well as carrying out a series of *in vivo* experiments that should show whether the observations described above correspond to the situation in living cells. Our current findings indicate that the repair of oxidative damage in vertebrate cells is highly regulated to prevent genomic instability, and future experiments should show how this regulation is mediated at the molecular level.

Acknowledgments—We are grateful to Mariela Artola-Borán for preparation of the phagemid substrates, Marie-Christine Weller for critical reading of the manuscript, Barbara van Loon for the gift of OGG1-GST and the bacterial MYH-GST expression vector, and to Yusaku Nakabeppu for the generous gift of the anti-MTH1 antibody.

REFERENCES

1. Jiricny, J. (2006) The multifaceted mismatch-repair system. *Nat. Rev. Mol. Cell Biol.* **7,** 335–346
2. Lahue, R. S., and Modrich, P. (1988) Methyl-directed DNA mismatch repair in *Escherichia coli*. *Mutat. Res.* **198,** 37–43
3. Modrich, P., and Lahue, R. (1996) Mismatch repair in replication fidelity, genetic recombination, and cancer biology. *Annu. Rev. Biochem.* **65,** 101–133
4. Peña-Diaz, J., and Jiricny, J. (2010) PCNA and MutLα: partners in crime in triplet repeat expansion? *Proc. Natl. Acad. Sci. U.S.A.* **107,** 16409–16410
5. Pluciennik, A., Dzantiev, L., Iyer, R. R., Constantin, N., Kadyrov, F. A., and Modrich, P. (2010) PCNA function in the activation and strand direction of MutLα endonuclease in mismatch repair. *Proc. Natl. Acad. Sci. U.S.A.* **107,** 16066–16071
6. Neuberger, M. S., Di Noia, J. M., Beale, R. C., Williams, G. T., Yang, Z., and Rada, C. (2005) Somatic hypermutation at A·T pairs: polymerase error versus dUTP incorporation. *Nat. Rev. Immunol.* **5,** 171–178
7. Schanz, S., Castor, D., Fischer, F., and Jiricny, J. (2009) Interference of mismatch and base excision repair during the processing of adjacent U/G mispairs may play a key role in somatic hypermutation. *Proc. Natl. Acad. Sci. U.S.A.* **106,** 5593–5598
8. Dianov, G. L., and Hübscher, U. (2013) Mammalian base excision repair: the forgotten archangel. *Nucleic Acids Res.* **41,** 3483–3490
9. Ghodgaonkar, M. M., Lazzaro, F., Olivera-Pimentel, M., Artola-Borán, M., Cejka, P., Reijns, M. A., Jackson, A. P., Plevani, P., Muzi-Falconi, M., and Jiricny, J. (2013) Ribonucleotides misincorporated into DNA act as strand-discrimination signals in eukaryotic mismatch repair. *Mol. Cell* **50,** 323–332
10. Collins, A. R. (1999) Oxidative DNA damage, antioxidants, and cancer. *BioEssays* **21,** 238–246
11. Gedik, C. M., and Collins, A. (2005) Establishing the background level of base oxidation in human lymphocyte DNA: results of an interlaboratory validation study. *FASEB J.* **19,** 82–84
12. Burrows, C. J., and Muller, J. G. (1998) Oxidative nucleobase modifications leading to strand scission. *Chem. Rev.* **98,** 1109–1152
13. David, S. S., O'Shea, V. L., and Kundu, S. (2007) Base-excision repair of oxidative DNA damage. *Nature* **447,** 941–950
14. McAuley-Hecht, K. E., Leonard, G. A., Gibson, N. J., Thomson, J. B., Watson, W. P., Hunter, W. N., and Brown, T. (1994) Crystal structure of a DNA duplex containing 8-hydroxydeoxyguanine-adenine base pairs. *Biochemistry* **33,** 10266–10270
15. Shibutani, S., Takeshita, M., and Grollman, A. P. (1991) Insertion of spe-

cific bases during DNA synthesis past the oxidation-damaged base 8-oxodG. *Nature* **349,** 431–434
16. Avkin, S., and Livneh, Z. (2002) Efficiency, specificity and DNA polymerase-dependence of translesion replication across the oxidative DNA lesion 8-oxoguanine in human cells. *Mutat. Res.* **510,** 81–90
17. Einolf, H. J., and Guengerich, F. P. (2001) Fidelity of nucleotide insertion at 8-oxo-7,8-dihydroguanine by mammalian DNA polymerase δ. Steady-state and pre-steady-state kinetic analysis. *J. Biol. Chem.* **276,** 3764–3771
18. Sakumi, K., Furuichi, M., Tsuzuki, T., Kakuma, T., Kawabata, S., Maki, H., and Sekiguchi, M. (1993) Cloning and expression of cDNA for a human enzyme that hydrolyzes 8-oxo-dGTP, a mutagenic substrate for DNA synthesis. *J. Biol. Chem.* **268,** 23524–23530
19. Maki, H., and Sekiguchi, M. (1992) MutT protein specifically hydrolyses a potent mutagenic substrate for DNA synthesis. *Nature* **355,** 273–275
20. Mo, J. Y., Maki, H., and Sekiguchi, M. (1992) Hydrolytic elimination of a mutagenic nucleotide, 8-oxodGTP, by human 18-kilodalton protein: sanitization of nucleotide pool. *Proc. Natl. Acad. Sci. U.S.A.* **89,** 11021–11025
21. Michaels, M. L., and Miller, J. H. (1992) The GO system protects organisms from the mutagenic effect of the spontaneous lesion 8-hydroxyguanine (7,8-dihydro-8-oxoguanine). *J. Bacteriol.* **174,** 6321–6325
22. Fortini, P., Pascucci, B., Parlanti, E., D'Errico, M., Simonelli, V., and Dogliotti, E. (2003) 8-Oxoguanine DNA damage: at the crossroad of alternative repair pathways. *Mutat. Res.* **531,** 127–139
23. Ohtsubo, T., Nishioka, K., Imaiso, Y., Iwai, S., Shimokawa, H., Oda, H., Fujiwara, T., and Nakabeppu, Y. (2000) Identification of human MutY homolog (hMYH) as a repair enzyme for 2-hydroxyadenine in DNA and detection of multiple forms of hMYH located in nuclei and mitochondria. *Nucleic Acids Res.* **28,** 1355–1364
24. Ushijima, Y., Tominaga, Y., Miura, T., Tsuchimoto, D., Sakumi, K., and Nakabeppu, Y. (2005) A functional analysis of the DNA glycosylase activity of mouse MUTYH protein excising 2-hydroxyadenine opposite guanine in DNA. *Nucleic Acids Res.* **33,** 672–682
25. van Loon, B., and Hübscher, U. (2009) An 8-oxo-guanine repair pathway coordinated by MUTYH glycosylase and DNA polymerase λ. *Proc. Natl. Acad. Sci. U.S.A.* **106,** 18201–18206
26. Dufner, P., Marra, G., Räschle, M., and Jiricny, J. (2000) Mismatch recognition and DNA-dependent stimulation of the ATPase activity of hMutSα is abolished by a single mutation in the hMSH6 subunit. *J. Biol. Chem.* **275,** 36550–36555
27. Koi, M., Umar, A., Chauhan, D. P., Cherian, S. P., Carethers, J. M., Kunkel, T. A., and Boland, C. R. (1994) Human chromosome 3 corrects mismatch repair deficiency and microsatellite instability and reduces N-methyl-N′-nitro-N-nitrosoguanidine tolerance in colon tumor cells with homozygous hMLH1 mutation. *Cancer Res.* **54,** 4308–4312
28. Iaccarino, I., Marra, G., Palombo, F., and Jiricny, J. (1998) hMSH2 and hMSH6 play distinct roles in mismatch binding and contribute differently to the ATPase activity of hMutSα. *EMBO J.* **17,** 2677–2686
29. Kubota, Y., and Takisawa, H. (1993) Determination of initiation of DNA replication before and after nuclear formation in *Xenopus* egg cell free extracts. *J. Cell Biol.* **123,** 1321–1331
30. Baerenfaller, K., Fischer, F., and Jiricny, J. (2006) Characterization of the "mismatch repairosome" and its role in the processing of modified nucleosides *in vitro*. *Methods Enzymol.* **408,** 285–303
31. Modrich, P. (2006) Mechanisms in eukaryotic mismatch repair. *J. Biol. Chem.* **281,** 30305–30309
32. Jacobs, A. L., and Schär, P. (2012) DNA glycosylases: in DNA repair and beyond. *Chromosoma* **121,** 1–20
33. Dianov, G., Price, A., and Lindahl, T. (1992) Generation of single-nucleotide repair patches following excision of uracil residues from DNA. *Mol. Cell. Biol.* **12,** 1605–1612
34. Frosina, G., Fortini, P., Rossi, O., Carrozzino, F., Raspaglio, G., Cox, L. S., Lane, D. P., Abbondandolo, A., and Dogliotti, E. (1996) Two pathways for base excision repair in mammalian cells. *J. Biol. Chem.* **271,** 9573–9578
35. Klungland, A., and Lindahl, T. (1997) Second pathway for completion of human DNA base excision-repair: reconstitution with purified proteins and requirement for DNase IV (FEN1). *EMBO J.* **16,** 3341–3348
36. Fang, W. H., and Modrich, P. (1993) Human strand-specific mismatch repair occurs by a bidirectional mechanism similar to that of the bacterial reaction. *J. Biol. Chem.* **268,** 11838–11844
37. Thomas, D. C., Roberts, J. D., and Kunkel, T. A. (1991) Heteroduplex repair in extracts of human HeLa cells. *J. Biol. Chem.* **266,** 3744–3751
38. Mazurek, A., Berardini, M., and Fishel, R. (2002) Activation of human MutS homologs by 8-oxo-guanine DNA damage. *J. Biol. Chem.* **277,** 8260–8266
39. Larson, E. D., Iams, K., and Drummond, J. T. (2003) Strand-specific processing of 8-oxoguanine by the human mismatch repair pathway: inefficient removal of 8-oxoguanine paired with adenine or cytosine. *DNA Repair* **2,** 1199–1210
40. Holmes, J., Jr., Clark, S., and Modrich, P. (1990) Strand-specific mismatch correction in nuclear extracts of human and *Drosophila melanogaster* cell lines. *Proc. Natl. Acad. Sci. U.S.A.* **87,** 5837–5841
41. Kadyrov, F. A., Dzantiev, L., Constantin, N., and Modrich, P. (2006) Endonucleolytic function of MutLα in human mismatch repair. *Cell* **126,** 297–308
42. Peña-Diaz, J., Bregenhorn, S., Ghodgaonkar, M., Follonier, C., Artola-Borán, M., Castor, D., Lopes, M., Sartori, A. A., and Jiricny, J. (2012) Non-canonical mismatch repair as a source of genomic instability in human cells. *Mol. Cell* **47,** 669–680
43. Boldogh, I., Milligan, D., Lee, M. S., Bassett, H., Lloyd, R. S., and McCullough, A. K. (2001) hMYH cell cycle-dependent expression, subcellular localization and association with replication foci: evidence suggesting replication-coupled repair of adenine:8-oxoguanine mispairs. *Nucleic Acids Res.* **29,** 2802–2809
44. Gillespie, P. J., Gambus, A., and Blow, J. J. (2012) Preparation and use of *Xenopus* egg extracts to study DNA replication and chromatin associated proteins. *Methods* **57,** 203–213
45. Brooks, P., Dohet, C., Almouzni, G., Méchali, M., and Radman, M. (1989) Mismatch repair involving localized DNA synthesis in extracts of *Xenopus* eggs. *Proc. Natl. Acad. Sci. U.S.A.* **86,** 4425–4429
46. Nash, H. M., Bruner, S. D., Schärer, O. D., Kawate, T., Addona, T. A., Spooner, E., Lane, W. S., and Verdine, G. L. (1996) Cloning of a yeast 8-oxoguanine DNA glycosylase reveals the existence of a base-excision DNA-repair protein superfamily. *Curr. Biol.* **6,** 968–980
47. Dherin, C., Radicella, J. P., Dizdaroglu, M., and Boiteux, S. (1999) Excision of oxidatively damaged DNA bases by the human α-hOgg1 protein and the polymorphic α-hOgg1(Ser326Cys) protein which is frequently found in human populations. *Nucleic Acids Res.* **27,** 4001–4007
48. Warren, J. J., Pohlhaus, T. J., Changela, A., Iyer, R. R., Modrich, P. L., and Beese, L. S. (2007) Structure of the human MutSα DNA lesion recognition complex. *Mol. Cell* **26,** 579–592
49. Colussi, C., Parlanti, E., Degan, P., Aquilina, G., Barnes, D., Macpherson, P., Karran, P., Crescenzi, M., Dogliotti, E., and Bignami, M. (2002) The mammalian mismatch repair pathway removes DNA 8-oxodGMP incorporated from the oxidized dNTP pool. *Curr. Biol.* **12,** 912–918
50. Russo, M. T., Blasi, M. F., Chiera, F., Fortini, P., Degan, P., Macpherson, P., Furuichi, M., Nakabeppu, Y., Karran, P., Aquilina, G., and Bignami, M. (2004) The oxidized deoxynucleoside triphosphate pool is a significant contributor to genetic instability in mismatch repair-deficient cells. *Mol. Cell. Biol.* **24,** 465–474
51. Gu, Y., Parker, A., Wilson, T. M., Bai, H., Chang, D. Y., and Lu, A. L. (2002) Human MutY homolog, a DNA glycosylase involved in base excision repair, physically and functionally interacts with mismatch repair proteins human MutS homolog 2/human MutS homolog 6. *J. Biol. Chem.* **277,** 11135–11142
52. Hashimoto, Y., Ray Chaudhuri, A., Lopes, M., and Costanzo, V. (2010) Rad51 protects nascent DNA from Mre11-dependent degradation and promotes continuous DNA synthesis. *Nat. Struct. Mol. Biol.* **17,** 1305–1311